

Kinetic theory of cosmic ray and gamma-ray production in supernova remnants expanding into wind bubbles

Evgeny G. Berezhko¹ and Heinrich J. Völk²

¹ Institute of Cosmophysical Research and Aeronomy, Lenin Ave. 31, 677891 Yakutsk, Russia
 email: berezhko@sci.yakutia.ru

² Max-Planck-Institut für Kernphysik, Postfach 103980, D-69029 Heidelberg, Germany
 email: Heinrich.Voelk@mpi-hd.mpg.de

Received 103 December 1999; / Accepted 1 date;

Abstract. A kinetic model of particle acceleration in supernova remnants (SNRs) is extended to study the cosmic ray (CR) and associated high-energy γ -ray production during SN shock propagation through the inhomogeneous circumstellar medium of a progenitor star that emits a wind. The wind forms a low-density bubble surrounded by a swept-up shell of interstellar matter. γ -rays are produced as a result of decay of pions which in turn are the result of collisions of CRs with nuclei of the thermal plasma. The time evolution of the SNRs is followed numerically, taking into account the nonlinear backreaction of the accelerated CRs. The model for SNRs includes injection of suprathermal particles at the shock front and heating of the thermal plasma due to dissipation of Alfvén waves in the precursor region. Examples typical for SN type Ib and SN type II explosions are considered. Apart from the confirmation of the known fact that acceleration is extremely rapid and that the upper momentum cutoff is reached almost immediately after the explosion due to the high wind magnetic field, it is also shown that the CRs are accelerated with a high efficiency. Depending on the circumstellar parameters, 20% to 40% of the SN explosion energy is absorbed by CRs during the SNR evolution for a moderate injection rate, when a fraction $\eta = 10^{-3}$ of the gas particles, swept up by the supernova shock, is accelerated. The CR momentum spectrum, ultimately produced in the SNRs, has a power law form $N \propto p^{-\gamma}$ with an index $\gamma = 2.0$ to 2.1 in a wide energy range up to a maximum energy, which is about 10^{14} eV, if the CR diffusion coefficient is as small as the Bohm limiting value. It is to be expected that the resulting CR chemical composition at high energies reflects more the stellar wind composition, whereas at lower energies it corresponds more to that of the average interstellar medium. The expected π^0 -decay γ -ray flux is however considerably lower than in the case of a uniform interstellar medium; a relatively high γ -ray luminosity in the band $\epsilon_\gamma \gtrsim 1$ TeV, detectable at distances of several kpc, is only expected in the case of a relatively dense ISM with

a number density above 10 cm^{-3} . Extremely high γ -ray emission may be produced when the SN shock propagates through the slow dense wind of a red supergiant, the progenitor of a SN type II. In this case SNRs might be visible in γ -rays for several hundred years out to distances of tens of kpc. For the case of a SN type Ib the expected π^0 -decay γ -ray TeV-energy flux during the whole SNR evolution remains lower than $10^{-11} \text{ cm}^{-2}\text{s}^{-1}$ if the interstellar number density is less than 0.3 cm^{-3} .

Key words: supernova: general – cosmic rays – shock acceleration – γ -rays

1. Introduction

Considerable efforts have been made during the last years to empirically confirm the theoretical expectation that the main part of the Galactic cosmic rays (CRs) originates in supernova remnants (SNRs). Theoretically progress in the solution of this problem has been due to the development of the theory of diffusive shock acceleration (see, for example, reviews by Drury 1983; Blandford & Eichler 1987; Berezhko & Krymsky 1988). Although still incomplete, the theory is able to explain the main characteristics of the observed CR spectrum under several reasonable assumptions, at least up to an energy of $10^{14} \div 10^{15}$ eV. Direct information about the dominant nucleonic CR component in SNRs can only be obtained from γ -ray observations. If this nuclear component is strongly enhanced inside SNRs then through inelastic nuclear collisions, leading to pion production and subsequent decay, γ -rays will be produced.

CR acceleration in SNRs expanding in a uniform interstellar medium (ISM) (Drury et al. 1989; Markiewicz et al. 1990; Dorfi 1990), and the properties of the associated γ -ray emission (Dorfi 1991; Drury et al. 1994) were investigated in a number of studies (we mention here only those papers which include the effects of shock geometry and time-dependent nonlinear CR backreaction; for a review of others which deal with the test particle approximation,

see for example Drury 1983; Blandford & Eichler 1987; Berezhko & Krymsky 1988; Völk 1997). All of these studies are based on a two-fluid hydrodynamical approach and directly employ the assumption that the expanding SN shock is locally plane; as dynamic variables for the CRs the pressure and the energy density are determined. Their characteristics are sometimes essentially different from the results obtained in a kinetic approach (Kang & Jones 1991; Berezhko et al. 1994, 1995, 1996) which consistently takes the role of shock geometry and nonlinear CR backreaction into account. First of all, in kinetic theory the form of the spectrum of accelerated CRs and their maximum energy are calculated selfconsistently. In particular, the maximum particle energy ϵ_{max} , achieved at any given evolutionary stage, is determined by geometrical factors (Berezhko 1996), in contrast to the hydrodynamic models which in fact postulate that the value of $\epsilon_{max}(t)$ is determined by the time interval t that has passed since the explosion (Drury et al. 1989; Markiewicz et al. 1990; Dorfi 1990; Jones & Kang 1992). Although the difference between the values of ϵ_{max} in the two cases is not very large, it critically influences the structure and evolution of the shock. For example, the shock never becomes completely modified (smoothed) by the CR backreaction (Kang & Jones 1991; Berezhko et al. 1994, 1995, 1996). Together with the smooth precursor, the shock transition always contains a relatively strong subshock which heats the swept-up gas and leads to the injection of suprathermal gas particles into the acceleration process. In this sense diffusive shock acceleration is somewhat less efficient than predicted by hydrodynamic models. Acceleration always requires some freshly injected particles which are generated during gas heating. This prediction is in agreement with the observations that show significant gas heating in young SNRs.

On the other hand, the shock modification by the CR backreaction is even greater than predicted by hydrodynamic models. The total shock compression ratio $\sigma \propto M^{3/4}$ (Berezhko et al. 1996) is a monotonically rising function of the shock Mach number M and can significantly exceed the classical value 4, or even the value $\sigma = 7$ that corresponds to a postshock medium dominated by relativistic CRs. This result is a direct consequence of the fact that CR acceleration at the front of a spherically expanding shock is accompanied by a temporally increasing dilution of shock energy in the form of CRs in the precursor region (Drury et al. 1995; Berezhko 1996). Qualitatively this leads to the same effect as if energetic particles or thermal gas energy were radiated away from the shock (Berezhko 1996; Berezhko & Ellison 1999). We note that this energy dilution effect is much stronger than the effect of a decreasing specific heat ratio due to the conversion of shock energy into relativistic CRs.

The additional gas heating in the precursor region due to Alfvén wave dissipation significantly restricts the shock compression ratio $\sigma(t)$ even though its value still considerably exceeds 4 for a strong shock (Berezhko et al. 1996;

Berezhko & Völk 1997). The precursor gas heating has a much less pronounced effect in the hydrodynamic description (e.g. Dorfi 1990).

As far as the expected γ -ray emission, produced in SNRs by the nuclear CR component, is concerned, there are less significant differences between the kinetic (Berezhko & Völk 1997) and the hydrodynamic (Dorfi 1991; Drury et al. 1994) predictions, even though these differences are not unimportant. The reason is that the peak value of the γ -ray flux is mainly determined by the fraction of overall hydrodynamic explosion energy that is transferred to CRs, i.e. by the overall efficiency of CR acceleration which is not strongly dependent on the model used.

The differences in the time variation of the predicted γ -ray fluxes are more essential. Kinetic theory (Berezhko & Völk 1997) revealed much more effective CR and γ -ray production during the free expansion phase. It also shows a more rapid decrease of the γ -ray flux during the subsequent Sedov phase after reaching its peak value, due to the different spatial distributions of thermal gas and CRs inside SNRs. This energy-dependent lack of overlap is not taken into account in hydrodynamic models.

The model developed by Ellison and co-workers to describe diffusive shock acceleration of CRs and to predict the expected γ -ray emission from SNRs, uses a Monte Carlo (MC) simulation of pitch angle scattering. It is applied in the same way to all particles, both CR and thermal particles, and is correspondingly solved numerically from the outset (e.g. Ellison et al. 1995; Baring et al. 1999). The energetic particle population (i.e. accelerated CRs) naturally arises in this approach as a high energy tail of the distribution of gas particles which undergo heating in the strongest gradient of the selfconsistently modified shock transition, the subshock in our notation. In this way the model incorporates not only selfconsistent CR acceleration but also gas heating and particle injection into the acceleration process. Since it is a plane-wave steady state model it includes as a free parameter the value of the CR cutoff energy ϵ_{max} , which can not be calculated in this kind of model. On the other hand, at sufficiently high particle energies the description corresponds to a diffusive approach based on the diffusive transport equation. Therefore our time-dependent kinetic description in spherical symmetry, with an injection rate that corresponds to the MC-model, and the MC-model, in turn incorporating the same value of CR cutoff energy, give identical CR spectra at any stage of the free expansion phase for the same set of ISM and shock parameters (Berezhko & Ellison 2000). This means that in its free expansion phase the SNR evolution can be represented as a sequence of quasi-stationary states; each of them can be reproduced in the framework of the plane-wave steady state description with the corresponding value of the CR cutoff energy $\epsilon_{max}(t)$. The situation becomes more complicated in the subsequent Sedov phase due to the existence of a so-

called escaping particle population near the shock front (Berezhko & Ellison 1999b), which is a purely nonstationary phenomenon (Berezhko 1986a; Berezhko & Krymsky 1988) and therefore can not be reproduced in the framework of a steady state approach. As far as the overall CR spectrum and the associated γ -ray flux at any given evolutionary phase are concerned, the plane wave description can only give an approximate estimate because it does not include such important physical factors as CR adiabatic cooling and the incomplete overlap of the spatial distributions of gas and CRs inside the expanding SNR.

The evolution of SNRs in a uniform ISM is typical only for SNe type Ia. SNe of type Ib and II, which are more numerous in our Galaxy, explode into an inhomogeneous circumstellar medium, formed by the intensive wind of their massive progenitor stars (Losinskaya 1991). This is at least true for progenitor masses $M \gtrsim 20M_{\odot}$ whose main sequence winds are very energetic. Their time-integrated hydrodynamic energy output is so large that they create wind cavities which are about as large as the size of a remnant of the subsequent Supernova explosion, if it would occur in a uniform ISM of the same density. The more frequent lower mass core collapse progenitors ($8 \lesssim M \lesssim 20M_{\odot}$) have at least a massive Red Supergiant wind region before the transition to the external ISM. Therefore the description of SNR evolution and CR acceleration becomes considerably more difficult for those cases. Due to the complicated structure of the medium one can expect that the difference between kinetic and hydrodynamic model predictions will be even more pronounced than in the case of a uniform ISM.

Up to now, except for the paper by Berezhko & Völk (1995) where preliminary results of the present work were presented, the consideration of CR acceleration in the case of a SN type Ib and SN type II was considered only for SN shock propagation through the region of the supersonic stellar wind (Berezinskii & Ptuskin 1988; Völk & Biermann 1988; Jones & Kang 1992; Kirk et al. 1995). Since this region is characterized by an initially very strong if spatially decreasing magnetic field of stellar origin and a very high shock speed, the maximum energy of CRs accelerated in the wind region is achieved extremely rapidly during a period of time comparable with the SNR age at each phase, and then it remains nearly constant due to a balance of acceleration gains and adiabatic losses (Völk & Biermann 1988). As it is shown below, the expected CR energy spectrum is close to being selfsimilar where the amplitude monotonically decreases with time but the shape remains invariant (see Appendix). Thus the situation is very different from that for a uniform circumstellar medium with a standard magnitude ISM field strength, where the maximum CR energy is only achieved at the end of the sweep-up phase, after hundreds or even thousands of years.

The direct dependence on the stellar surface field also raised hopes that the CR acceleration in the wind would

constitute a major source of the observed Galactic CRs with energies $\epsilon \gtrsim 10^{14}$ eV. The most optimistic assumptions predict CR generation in these regions up to an energy of 3×10^{18} eV (Biermann 1993). In this context we would like to make the following remarks:

First of all, the supersonic wind region contains a relatively small amount of mass $M \lesssim 1M_{\odot}$ which is typically smaller than the ejected mass $M_{ej} \sim 10M_{\odot}$. Therefore the fraction of the SN explosion energy which can be transferred into CRs is typically lower than required for the observed CR spectrum, especially in the case of a SN type Ib (see below).

Second, to achieve a particle energy significantly greater than 10^{14} eV one needs to assume an unusually high magnetic field in the wind. This tends to violate the condition $V_w \geq c_a$, necessary for the existence of a supersonic flow in the first place, as pointed out by Axford (1994), where V_w is the wind speed and c_a is the Alfvén velocity.

Third, the wind magnetic field is largely azimuthal, except in the very polar region near the stellar rotation axis, and the outer SNR shock is almost perpendicular. Therefore not only the suprathermal ion injection is much less efficient but also the CR acceleration itself appears not so efficient as in the case of a quasi-parallel shock. Although one can give some physical arguments which assert that particle injection with their subsequent acceleration takes place also in this case, one needs a more rigorous treatment of this complex question. An example for the acceleration at a shock propagating through a stationary stochastic large *yscale* magnetic field that is on average perpendicular to the shock normal is given by Kirk et al. (1996) based on the process of anomalous diffusion (see Chuvilgin & Ptuskin 1993). This test particle calculation indicates, as intuitively expected, that the spectrum of accelerated particles is steeper than for acceleration at a quasi-parallel shock. As a consequence, the nonlinear efficiency of acceleration would also have to be assumed to be significantly reduced.

Fourth, the unusually high maximum CR energy predicted by Biermann (1993) is a direct consequence of the assumption of a very small and energy independent CR diffusion coefficient, presumably produced by the chaotic turbulent motions of the medium near the shock, that formally gives very fast acceleration to extremely high energies. Leaving aside the important question concerning the justification of the assumption for such shock-produced turbulent motions also significantly ahead of the forward SNR shock itself (see e.g. Ellison et al. 1994, Lucek & Bell 2000), one has to stress that the final result should in any case depend upon the values of the microscopic CR diffusion tensor which alone allows CRs to intersect the shock front many times with a subsequent increase of their energy. As far as the macroscopic CR diffusion due to chaotic gas motions (Biermann 1993) is concerned, it can not itself provide CR acceleration. In fact, from what

has been said before, even our results presented below, based on the usual assumption about Bohm type microscopic particle diffusion in a quasi-parallel shock and much less optimistic compared with those in Biermann (1993), must be considered as an upper limit for the CR energy density which can be achieved during shock acceleration. This leaves open the question whether the evolving SNR shock system can generate a strong scattering wave field and allows the assumption of a favorable ratio of the microscopic parallel and perpendicular diffusion coefficients over a sufficiently long time, so that the maximum individual particle energy can be increased by something like an order of magnitude or more for a perpendicular shock (Jokipii 1987; Ostrowski 1988; Ellison et al. 1995; Reynolds 1998).

As mentioned above, a strong wind modifies the environment of massive progenitors of SN types Ib and II. It sweeps up the ambient gas into a thin shell surrounding a rarefied bubble (Weaver et al. 1977; Losinskaya 1991). Since the typical cavity is greater than 10 pc in size and contains a considerable amount of matter, it can significantly influence the SNR evolution and CR acceleration. Estimates and preliminary numerical calculations indicate that the SN shock propagation through the progenitor's wind region should generate high-energy π^0 -decay γ -ray emission on a detectable level (Berezinsky & Ptuskin 1988; Kirk et al. 1995; Berezhko & Völk 1995¹). Yet, up to now, all *detailed* numerical investigations of CR acceleration in SNRs have dealt with the case of a star exploding into a uniform homogeneous medium.

In this paper we present a detailed extension of the kinetic model for CR acceleration in SNRs (Berezhko et al. 1994, 1995, 1996; Berezhko & Völk 1997) to the case of a nonuniform circumstellar medium, spherical symmetry still being assumed. We study the CR acceleration and π^0 -decay γ -ray production taking into account that the circumstellar medium can be strongly modified by a wind from the progenitor star. In doing this we assume energetic particle scattering governed by the Bohm diffusion coefficient in the local mean magnetic field, treating the shock normal to be quasi-parallel to the field direction. We have studied two cases typical for type Ib and type II SNe. In the first case, a star with an initial mass of $35 M_\odot$ at the end of its evolution explodes as SN into the cavity created by a main-sequence (MS) O-star wind and the subsequent winds during the red supergiant (RSG) and Wolf-Rayet (WR) phases. For the case of a SN type II we take the example of the explosion of a star with initial mass $15 M_\odot$ into the cavity created by the winds emitted during the MS and RSG phases. In both cases we consider

¹ Due to an error in the plot routine in Fig. 1 of Berezhko & Völk (1995), the γ -ray fluxes in the wind SNR cases were plotted with an enlargement factor of 2500 which should be left out.

the two different interstellar number densities 0.3 and 30 cm⁻³.

We shall not address here the question of γ -ray production by electron synchrotron emission, Bremsstrahlung, or the inverse Compton (IC) effect on ambient low energy photons. Especially at very high energies exceeding ~ 10 GeV, IC γ -rays appear to dominate the emission from plerions like the Crab nebula (e.g. de Jager & Harding 1992, Atoyan & Aharonian 1996), where presumably a relativistic wind of electron-positron pairs from the pulsar is dissipated in a circumstellar termination shock deep inside the SNR shell. The IC effect associated with acceleration of ultrarelativistic electrons inside the SNR shell, or at its leading shock (along with ions considered here), may also contribute quantitatively to the γ -ray luminosity of a SNR as simple estimates suggest (Mastichiadis 1996; Mastichiadis & de Jager 1996). Therefore in any specific source this leptonic contribution to the γ -ray flux needs to be estimated before the hadronic π^0 -decay γ -ray emission can be compared with the theoretical models presented below.

We briefly describe some aspects of the model in Sect. 2 since it was in detail described in a previous paper (Berezhko & Völk 1997). Sect. 3 contains the results and Sect. 4 includes the discussion and the conclusions.

2. Model

2.1. CR acceleration and SNR evolution

During the early phase of SNR evolution the hydrodynamical SN explosion energy E_{sn} is kinetic energy of the expanding shell of ejected mass. The motion of these ejecta produces a strong shock wave in the background medium, whose size R_s increases with velocity $V_s = dR_s/dt$. Diffusive propagation of energetic particles in the collisionless scattering medium allows them to traverse the shock front many times. Each two subsequent shock crossings increase the particle energy. In plane geometry this diffusive shock acceleration process (Krymsky 1977; Axford et al. 1977; Bell 1978; Blandford & Ostriker 1978) creates a power law-type CR momentum spectrum. Due to their large energy content the CRs can dynamically modify the shock structure.

The description of CR acceleration by a spherical SNR shock wave is based on the diffusive transport equation for the CR distribution function $f(r, p, t)$ (Krymsky 1964; Parker 1965):

$$\frac{\partial f}{\partial t} = \frac{1}{r^2} \frac{\partial}{\partial r} r^2 \kappa \frac{\partial f}{\partial r} - w_c \frac{\partial f}{\partial r} + \frac{1}{r^2} \frac{\partial}{\partial r} (r^2 w_c) \frac{p}{3} \frac{\partial f}{\partial p} + Q, \quad (1)$$

where Q is the source term due to injection; r , t and p denote the radial coordinate, the time, and particle momentum, respectively; κ is the CR diffusion coefficient; $u = V_s - w$. In addition,

$$w_c = w \text{ for } r < R_s, \quad w_c = w + c_a \text{ for } r > R_s,$$

where w is the radial mechanical velocity of the scattering medium (i.e. thermal gas), c_a is the speed of forward Alfvén waves generated in the upstream region by the anisotropy of the accelerating CRs. In the downstream plasma the propagation directions of the scattering waves are assumed to be isotropized (e.g. Drury et al. 1989).

The thermal matter is described by the gas dynamic equations

$$\frac{\partial \rho}{\partial t} + \frac{1}{r^2} \frac{\partial}{\partial r} (r^2 \rho w) = 0, \quad (2)$$

$$\rho \frac{\partial w}{\partial t} + \rho w \frac{\partial w}{\partial r} = -\frac{\partial}{\partial r} (P_g + P_c), \quad (3)$$

$$\frac{\partial P_g}{\partial t} + w \frac{\partial P_g}{\partial r} + \frac{\gamma_g}{r^2} \frac{\partial}{\partial r} (r^2 w) P_g = \alpha_a (\gamma_g - 1) c_a \frac{\partial P_c}{\partial r}, \quad (4)$$

where ρ , γ_g and P_g denote the mass density, specific heat ratio and the pressure of gas, respectively, and

$$P_c = \frac{4\pi c}{3} \int_0^\infty dp \frac{p^4 f}{\sqrt{p^2 + m^2 c^2}} \quad (5)$$

is the CR pressure. These gas dynamic equations include the CR backreaction via term $-\partial P_c/\partial r$. They also describe the gas heating due to the dissipation of Alfvén waves in the upstream region (McKenzie & Völk 1982; Völk et al. 1984); it is given by the parameter $\alpha = 1$ at $r > R_s$ and $\alpha_a = 0$ at $r < R_s$.

We expect that the SNR shock always includes a sufficiently strong subshock which heats the gas and plays an important dynamical role, also in the present case of nonuniform background medium. The gas subshock, situated at $r = R_s$, is treated as a discontinuity on which all hydrodynamical quantities undergo a jump.

We assume, that the injection of some (small) fraction of gas particles into the acceleration process takes place at the subshock, that is described by the source

$$Q = Q_s \delta(r - R_s).$$

For the sake of simplicity we restrict our consideration to protons, which are the dominant ions in the cosmic plasma. At present we only have some experimental (e.g. Lee 1982; Trattner et al. 1994) and theoretical (Quest 1988; Trattner & Scholer 1991; Giacalone et al. 1993; Bennett & Ellison 1995; Malkov & Völk 1995, 1996) indications as to what value of the injection rate can be expected. We use here a simple CR injection model, in which a small fraction η of the incoming protons is instantly injected at the gas subshock with a speed $\lambda > 1$ times the postshock gas sound speed c_{s2} (Berezhko et al. 1990; Kang & Jones 1991; Berezhko et al. 1994, 1995, 1996; Berezhko & Völk 1997):

$$Q_s = \frac{u_1 N_{inj}}{4\pi p_{inj}^3} \delta(p - p_{inj}), \quad N_{inj} = \eta N_1, \quad p_{inj} = \lambda m c_{s2}, \quad (6)$$

where $N = \rho/m$ is the proton number density, and m is the particle (proton) mass. For simplicity, we always use $\lambda = 2$. The subscripts 1(2) refer to the point just ahead (behind) the subshock.

We assume that the Bohm diffusion coefficient is a good approximation for strong shocks (McKenzie & Völk 1982), characterized by strong wave generation (Bell 1978). This latter question has been studied very recently in its nonlinear consequences, by Lucek & Bell (2000) numerically, and by Bell & Lucek (2000) using an analytical model. The conclusion is that wave generation in very strong shocks should not only lead to Bohm diffusion, but also to an amplification of the pre-shock magnetic field that increases the acceleration rate, as had been speculated earlier (Völk 1984). We use here the CR diffusion coefficient

$$\kappa(p) = \rho_B c / 3, \quad (7)$$

where ρ_B is the gyroradius of a particle with momentum p in the magnetic field B , c is the speed of light. This coefficient differs from the Bohm diffusion coefficient in the non-relativistic energy region, but this difference is absolutely unimportant because of the very high acceleration rate at $p < mc$. In the disturbed region we use $\kappa = \kappa_s \rho_s / \rho$, where the subscript s corresponds to the current shock position $r = R_s$. An additional factor ρ_s / ρ was assumed to prevent the instability of the precursor (Drury 1984; Berezhko 1986b). It can also be interpreted as describing the enhancement of magnetic turbulence in a region of higher gas density.

Alfvén wave dissipation (Völk et al. 1984) as an additional heating mechanism strongly influences the structure of a modified shock in the case of large sonic Mach number $M = V_s / c_s \gg \sqrt{M_a}$, $M_a = V_s / c_a$ is the Alfvénic Mach number, c_s and c_a are the local sound and Alfvén speeds correspondingly, at the shock front position $r = R_s$. The wave damping substantially restricts the growth of the shock compression ratio $\sigma = \rho_2 / \rho_s$ at the level $\sigma \approx M_a^{3/8}$ which, in the absence of Alfvén wave dissipation, has been found to reach extremely high values $\sigma \approx M^{3/4}$ for large Mach numbers (Berezhko et al. 1996; Berezhko & Ellison 1999).

The dynamic equations are solved under the initial ($t = t_i$) conditions:

$$f(p) = 0, \quad \rho = \rho_0(r, t_w), \\ P_g = P_{g0}(r, t_w), \quad w = w_0(r, t_w), \quad (8)$$

which neglect the background CRs and describe some ambient gas distribution modified by the wind from the progenitor star emitted during a preceding time period t_w . The time $t = 0$ corresponds to the instant of SN explosion.

The result of a core collapse supernova, many days after the explosion, is freely expanding gas with velocity

$v = r/t$. The density profile of the ejecta is described by (Jones et al. 1981; Chevalier 1982; Chevalier & Liang 1989)

$$\rho_{ej} = \begin{cases} Ft^{-3}, & v < v_t \\ Ft^{-3}(v/v_t)^{-k}, & v \geq v_t, \end{cases} \quad (9)$$

where

$$F = \frac{1}{4\pi k} \frac{[3(k-3)M_{ej}]^{5/2}}{[10(k-5)E_{sn}]^{3/2}}, \quad v_t = \left[\frac{10(k-5)E_{sn}}{3(k-3)M_{ej}} \right]^{1/2},$$

M_{ej} is the total ejected mass. For SNRs the value of the parameter k typically lies between 7 and 12. The pressure in the expanding ejecta is negligible.

Interaction with the ambient material modifies the ejecta density distribution. We describe the ejecta dynamics in a simplified manner, assuming that the modified ejecta consist of two parts (Berezhko & Völk 1997): a thin shell (or piston) moving with some speed V_p and a freely expanding part which is described by the distribution (9). The piston includes the decelerated tail of the distribution (9) with initial velocities $v > R_p/t$, where R_p is the piston radius separating the ejecta and the swept-up ISM matter. The evolution of the piston is described in the framework of a simplified thin-shell approximation, in which the thickness of the shell is neglected. Behind the piston ($r < R_p$), the CR distribution is assumed to be uniform.

The high velocity tail in the distribution (9) ensures a large value of the SNR shock speed at an early phase of evolution. It increases the CR and γ -ray production significantly compared with the case where all the ejecta propagate with a single velocity (Berezhko & Völk 1997).

In the case of a uniform ISM it was shown that the CR penetration through the piston plays no important role for SN shock evolution and overall CR production (Berezhko et al. 1996). In the case of an intensive wind from the progenitor star, a relatively large volume around the progenitor is occupied by a low density bubble. The main amount of CRs and γ -rays are produced when the SNR shock interacts with this bubble. Piston and shock sizes are comparable and much larger than the dynamic scale of the system during the most effective CR production phase. Therefore one can expect that CR penetration through the piston is more important in comparison with the case of a uniform ISM.

The efficiency of diffusive CR penetration through the piston depends on the magnetic field structure, which is influenced by the Rayleigh-Taylor instability at the contact discontinuity ($r = R_p$) between the ejecta and the swept up medium that is contained in the region $R_p < r < R_s$. According to Chevalier's (1982) estimate, the energy density of the turbulent motions created by this instability is determined by the value of the thermal pressure P_p at the outer piston surface ($r = R_p + 0$), and may be as large as $e_t = 0.2P_p$. Turbulent motions in the ionized medium lead to the amplification of magnetic fields. We assume that the magnetic field grows up to the energy density

$e_B = 0.5e_t$. This turbulent magnetic field is presumably distributed over a wide range of length scales. The energy density of the magnetic field fluctuations which resonantly interact with particles in the momentum range from mc to p_m may be as large as $e_B/\ln(p_m/mc)$, which is about $0.1e_B$ for a typical CR cutoff momentum $p_m = 10^4mc$. Therefore we use a Bohm type diffusion coefficient in the piston region, corresponding to a magnetic field strength of $B = \sqrt{8\pi\delta P_p}$ with $\delta = 10^{-2}$.

Radiative gas cooling is not included in our model. This process becomes important at the late Sedov phase (Dorf 1991), when CR acceleration becomes inefficient.

Detailed descriptions of the model and of the numerical methods have been given earlier (Berezhko et al. 1994, 1995, 1996; Berezhko & Völk 1997).

2.2. Progenitor wind bubble

The strong wind from the massive progenitor star interacts with an ambient ISM of uniform density $\rho_0 = 1.4mN_H$, resulting to first approximation in an expanding spherical configuration, which is called a bubble (Weaver et al. 1977; Losinskaya 1991). Here m is the proton mass and N_H is the hydrogen number density in the background ISM where 10% of helium by number is assumed. Throughout its evolution, the system consists of four distinct zones. Starting from the center they are: (a) the hypersonic stellar wind (b) a region of shocked stellar wind (c) a shell of shocked interstellar gas, and (d) the ambient ISM.

We consider here the case of a so-called modified bubble whose structure is significantly influenced by mass transport from the dense and relatively cold shell (c) into the hot region (b), and by thermal conduction in the opposite direction, these two energy fluxes balancing each other to first order. During this stage the shell (c) has collapsed into a thin isobaric shell due to radiative cooling (Weaver et al. 1977; Kahn & Breitschwerdt 1989).

The sizes of each zone are determined by the ISM number density N_H , the wind speed V_w and the stellar mass-loss rate \dot{M} (Weaver et al. 1977), and can be written in the form:

$$R_1 = 4.38 \left(\frac{\dot{M}}{10^{-6}M_\odot/\text{yr}} \right)^{3/10} \times \left(\frac{V_w}{2000 \text{ km/s}} \right)^{1/10} \left(\frac{N_H}{1 \text{ cm}^{-3}} \right)^{-3/10} \left(\frac{t_w}{10^6 \text{ yr}} \right)^{2/5} \text{ pc} \quad (10)$$

is the inner shock radius which bounds the wind region (a);

$$R_2 = 27.5 \left(\frac{\dot{M}}{10^{-6}M_\odot/\text{yr}} \right)^{1/10} \times \left(\frac{V_w}{2000 \text{ km/s}} \right)^{4/10} \left(\frac{N_H}{1 \text{ cm}^{-3}} \right)^{-1/10} \left(\frac{t_w}{10^6 \text{ yr}} \right)^{3/5} \text{ pc} \quad (11)$$

is the outer shock radius which separates the shell (c) from the ISM. The time $t_w = 0$ corresponds to the onset of a steady, spherically symmetric stellar wind.

Region (a) is characterized by a negligibly small gas pressure P_g , a constant speed V_w , the gas density

$$\rho = \frac{\dot{M}}{4\pi V_w r^2} \quad (12)$$

and an essentially toroidal magnetic field (we use its value near the equatorial plane)

$$B = B_* \frac{R_* \Omega}{V_w} \frac{R_*}{r}, \quad (13)$$

where R_* is the radius and Ω the angular rotation rate of the star.

The regions (b) and (c) are isobaric with a thermal pressure (Weaver et al. 1977) that can be written in the form

$$P_b = 4.7 \times 10^{-12} \left(\frac{\dot{M}}{10^{-6} M_\odot/\text{yr}} \right)^{2/5} \left(\frac{V_w}{2000 \text{ km/s}} \right)^{4/5} \times \left(\frac{N_H}{1 \text{ cm}^{-3}} \right)^{3/5} \left(\frac{t_w}{10^6 \text{ yr}} \right)^{-4/5} \frac{\text{dyne}}{\text{cm}^2}. \quad (14)$$

The gas number density of the region (b) $N_b = \rho_b/m$ is approximately uniform and given by

$$N_b = 3.8 \times 10^{-2} \left(\frac{\dot{M}}{10^{-6} M_\odot/\text{yr}} \right)^{6/35} \left(\frac{N_H}{1 \text{ cm}^{-3}} \right)^{19/35} \times \left(\frac{V_w}{2000 \text{ km/s}} \right)^{12/35} \left(\frac{t_w}{10^6 \text{ yr}} \right)^{-22/35} \text{ cm}^{-3}. \quad (15)$$

The shell (c) is much denser: $N_c \gg N_b$. Therefore we can describe the number density distribution in regions (b) and (c) by the combined expression

$$N_g = \sigma_c N_0 \left(\frac{r}{R_2} \right)^{3(\sigma_c - 1)} + N_b, \quad (16)$$

where $N_0 = 1.4 N_H$, $\sigma_c N_0$ is the peak value of the shell number density reached at the front of the outer shock ($r = R_2 - 0$), and σ_c is the outer shock compression ratio.

The mass and heat transport between regions (b) and (c) are presumably due to turbulent motions in the bubble. We assume that the turbulent motions generate a magnetic field which grows up to the equipartition value

$$B_b = \sqrt{8\pi P_b}. \quad (17)$$

2.3. Gamma-ray production

π^0 -decay gamma rays are produced by energetic CR protons in inelastic collisions with gas nuclei which generate also neutral pions that subsequently decay. The γ -ray

emissivity of a SNR (in units of photons/s) can be written as (Drury et al. 1994)

$$Q_\gamma(\epsilon_\gamma) = 16\pi^2 \int_0^\infty dr r^2 \int_{p_\gamma}^\infty dp p^2 \sigma_{pp} Z_\gamma^\alpha c N_g f(r, p, t), \quad (18)$$

where

$$\sigma_{pp} = 38.5 + 0.46 \ln^2(0.01876p/\text{mc}) \text{ mb} \quad (19)$$

is the inelastic $p - p$ cross-section (e.g. Berezinsky et al. 1990), Z_γ^α is the so-called spectrum-weighted moment of the inclusive cross-section, p_γ is the momentum of a CR particle with kinetic energy $\epsilon = \epsilon_\gamma$, $N_g = \rho/m$ is the gas number density, $\alpha = 1 - d \ln n / d \ln \epsilon$ is the power law index of the integral CR energy spectrum, and $n = 4\pi p^2 f$ denotes the CR differential number density. We use the approximation for the spectrum-weighted moment as given by Drury et al. (1994), limiting Z_γ^α by the value

$$Z_\gamma^\alpha = \min\{0.2, 10^{1.49 - 2.73\alpha + 0.53\alpha^2}\} \quad (20)$$

The integral γ -ray flux at the distance d from the source is

$$F_\gamma(\epsilon_\gamma) = Q_\gamma(\epsilon_\gamma) / 4\pi d^2. \quad (21)$$

3. Results

Detailed investigations of CR acceleration and SNR evolution in a uniform ISM have revealed important features of this process (Berezhko et al. 1994, 1995, 1996; Berezhko & Völk 1997). For a wide range of injection rates the CR acceleration efficiency is very high, near unity, and therefore almost independent of the injection rate. Therefore we use here the particular value of the injection parameter $\eta = 10^{-3}$, which corresponds to a moderate injection rate for a parallel shock. This value of η implies an injection rate which is almost one order of magnitude lower than that resulting from simulations of collisionless plasma shocks (Quest 1988; Trattner & Scholer 1991; Giacalone et al. 1993), and which also corresponds to the kinetic MC model (e.g. Ellison et al. 1995; Baring et al. 1999) for parallel shocks. Our lower value of η effectively takes into account the influence of the average shock obliquity for a quasi-spherical SNR which expands into an ISM with a uniform mean magnetic field: according to Ellison et al. (1995), and Malkov & Völk (1995,) already at an angle $\theta \approx 45^\circ$ between the upstream magnetic field and the shock normal the injection rate is about an order of magnitude smaller than in the purely parallel shock case, if particle diffusion is somewhat less efficient than the Bohm limit. We can not exclude that even this effective injection rate leads to an overestimate for the global acceleration efficiency of the SNR.

We also restrict our consideration to a typical set of values of the SN parameters: hydrodynamic explosion energy $E_{sn} = 10^{51}$ erg, ejecta mass $M_{ej} = 10 M_\odot$, $k = 10$.

The radiative cooling of the swept-up shell of interstellar gas leads to high shell compression ratio $\sigma_c \gg 1$. The ISM magnetic field and the CRs which are produced by the outer shock can nevertheless significantly restrict this shell compression ratio. We use here the moderate value $\sigma_c = 10$. In fact, the final results are quite insensitive to the value of σ_c because the SN shock becomes an inefficient CR accelerator before reaching the region $r = R_2$ of the peak shell density.

3.1. Type Ib supernova

As a typical example for a type Ib SN we use theoretical results of stellar evolution with initial mass $35M_\odot$ (Garcia-Segura et al. 1996). According to these calculations the evolution consists of three stages: a MS phase with mass-loss rate $\dot{M} = 5.56 \times 10^{-7} M_\odot \text{ yr}^{-1}$, wind speed $V_w = 2000 \text{ km/s}$, and duration $\Delta t_w = 4.5 \times 10^6 \text{ yr}$; a RSG phase with $\dot{M} = 10^{-6} M_\odot \text{ yr}^{-1}$, $V_w = 15 \text{ km/s}$, $\Delta t_w = 2 \times 10^5 \text{ yr}$, and a WR-phase with $\dot{M} = 2.25 \times 10^{-5} M_\odot \text{ yr}^{-1}$, $V_w = 2000 \text{ km/s}$, and $\Delta t_w = 2 \times 10^5 \text{ yr}$.

According to Eq. (11) the MS wind creates a bubble of size $R_2 = 76.8 \text{ pc}$. The parameters of this modified bubble are $N_b = 5 \times 10^{-3} \text{ cm}^{-3}$, $P_b = 5.47 \times 10^{-13} \text{ dyne/cm}^2$.

The wind emitted during the RSG phase occupies a region of size $R_f = \Delta t_w V_w = 0.3 \text{ pc}$.

The fast wind from the subsequent WR star interacts with this dense RSG wind. After a relatively short period of time the WR wind breaks through the RSG wind material, leaving it in the form of clouds (Garcia-Segura et al. 1996). Taking into account that the interaction time is short and that the mass of the RSG wind is small compared with the bubble mass, we neglect in a zeroth approximation the influence of RSG phase on the final structure of the bubble.

Using again approximately Eqs. (11) and (15), the WR wind inside the MS-bubble now creates a WR bubble with number density $N_b = 1.02 \times 10^{-2} \text{ cm}^{-3}$ and a shell of size $R_2 = 56.2 \text{ pc}$. Formally this value N_b is twice as large as the number density of the MS bubble. If we disregard in our approximation the stellar mass lost in the WR phase compared to the mass of the partially swept-up MS bubble, the density of the new WR bubble can not exceed that of the MS bubble shell, simply for mass conservation. It can at best be equal if we assume that the WR shell is completely dissipated, i.e. smeared out over the WR bubble. This is in fact a quite reasonable assumption and we shall adopt it here. Therefore we use a simplified structure of the bubble, whose parameters $R_2 = 76.8 \text{ pc}$, $N_b = 5 \times 10^{-3} \text{ cm}^{-3}$, $P_b = 5.47 \times 10^{-13} \text{ dyne/cm}^2$, $B = 7.89 \mu\text{G}$ correspond to the MS-bubble, together with a hypersonic WR wind region of size $R_1 = 30.8 \text{ pc}$, corresponding to the pressure equilibrium condition $\rho V_w^2 = P_b$. This approximation to the dynamics is justified to the extent that we can neglect the overall mass lost by the star in comparison with the overall swept-up interstellar mass.

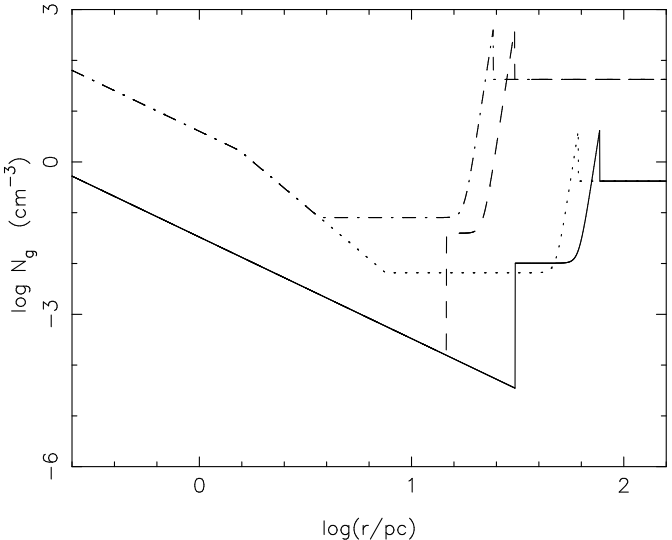


Fig. 1. Circumstellar gas density distribution as a function of radial distance for the case of a SNR Ib in an ISM with hydrogen number densities $N_H = 0.3 \text{ cm}^{-3}$ (full line) and $N_H = 30 \text{ cm}^{-3}$ (dashed line), and for the case of a SNR II with $N_H = 0.3 \text{ cm}^{-3}$ (dotted line) and $N_H = 30 \text{ cm}^{-3}$ (dash-dotted line).

The assumed circumstellar density distribution N_g is shown on Fig. 1 as a function of radial distance r for all the cases considered.

For the WR-star we use the parameters $R_* = 3 \times 10^{12} \text{ cm}$, $\Omega = 10^{-6}$, $B_* = 50 \text{ G}$, which determine the value of magnetic field in the wind region (a).

As we have already mentioned in the Introduction it is not obvious that our model (which is strictly speaking only valid for the case of a quasi-parallel shock) can be applied to the present case of a shock that is on average almost purely perpendicular. Basically it is not clear whether a sufficient number of suprathermal particles can be injected into a quasi-perpendicular shock (Ellison et al. 1995; Malkov & Völk 1995). On the other hand, there exist circumstances which should alleviate the obstacles for particle injection and their subsequent acceleration. One may assume that the magnetic field is essentially disordered on a spatial scale l_B , small compared with the main scale r . Over a substantial fraction of the magnetic flux tubes the SN shock will then be locally quasi-parallel, with particle injection and acceleration starting there without difficulties. If the scale l_B is larger than the diffusive length of suprathermal particles $l(p_{inj}) = \kappa_s(p_{inj})/V_s$, these particles will be at least accelerated up to the momentum p_* , where $l(p_*) \sim l_B$. If $l_B \gg l(p_{inj})$, accelerated particles with momenta $p_{inj} \leq p \leq p_*$ will gain a substantial part of the shock energy. In this case they can amplify magnetic field disturbances on progressively larger scales, that will allow another fraction of these particles to be further accelerated. Ultimately, some particles might indeed reach the maximum energy, which is determined by

the usual physical factors for a quasi-parallel shock (see below). However the particle spectrum is expected to be softer than for a quasi-parallel shock. For the suprathermal particles with energy $p_{inj} \sim mV_s$ the diffusive length is about $l \sim 10^{-6}R_s$. Therefore the above scenario will take place, if the magnetic field is initially disordered on a scale $l_B \gtrsim 10^{-4}r$, that seems not an unreasonable assumption.

We note, that there is some experimental evidence that particle (at least electron) diffusive shock acceleration in the progenitor wind actually takes place (see e.g. Chevalier 1982, Kirk et al. 1995, and references there).

We shall use here the assumption of Bohm type CR diffusion for a locally quasi-parallel shock. It implies an acceleration rate that is almost independent of the magnetic field structure. However, in the light of our above discussion of this field structure we consider our results as upper limits to the real CR and gamma-ray production efficiency.

Starting from some initial instant $t_i = R_{pi}/V_{pi} = 6.34$ yr after the SN explosion which corresponds to an initial piston position $R_{pi} = 3 \times 10^{17}$ cm and a piston speed $V_{pi} = 15 \times 10^3$ km/s, we explore the solution of the nonlinear dynamic equations following the SN shock propagation through the successive bubble zones. Note that the value of the initial position R_{pi} from which we start our calculations has as little physical importance as the short subsequent period of SNR evolution during which the quasi-stationary character of system evolution is established.

Fig. 2 illustrates the CR characteristics, SN shock parameters and expected γ -ray spectra produced during SN shock propagation through the supersonic WR wind region $r < R_1$.

In Fig. 2a the calculated CR distribution function at the subshock $f_s(p, t) = f(r = R_s, p, t)$ is presented for five different instants of time. The shape of the CR spectrum is determined by the fact that the shock is essentially modified by CR backreaction. Very soon after the beginning of CR acceleration the total shock compression ratio $\sigma = \rho_2/\rho_s$ reaches about $\sigma = 16.5$ and then slowly decreases with time. Although the total compression ratio is much higher than predicted by the hydrodynamical two-fluid model (Jones & Kang 1992), the subshock never disappears and its compression ratio remains nearly constant at the level $\sigma_s = \rho_2/\rho_1 \approx 3.4$ (see Fig. 2b). At small momenta $p_{inj} \leq p \lesssim mc$ the CR distribution function is almost a pure power-law $f_s \propto p^{-q_s}$ with the power-law index

$$q'_s = 3\sigma'_s/(\sigma'_s - 1), \quad (22)$$

determined by the effective subshock compression ratio $\sigma'_s = \sigma_s(1 - 1/M_{a1})$. At momenta $10 \text{ mc} \lesssim p \lesssim p_m$, where $p_m \sim 10^4 \text{ mc}$, the distribution function is also close to a power-law form $f_s \propto p^{-q}$ with the index value $q = 3.6$.

It is important to note, that our results confirm the conclusion that the accelerated particle spectrum can not be harder than $f \propto p^{-3.5}$ even for a very large shock compression ratio σ (Berezhko 1996; Malkov 1997; Berezhko & Ellison 1999a), whereas the test particle approach (see expression (27) below) in the case $\sigma \gg 1$ predicts the limiting value of the power law index $q = 3$.

An interesting point is that in the wind the CR distribution functions $f_s(p)$ at different evolutionary phases are almost selfsimilar to each other except during the initial short period $t < 10$ yr when the system undergoes the transition from the initial conditions at $t = t_i$ to the quasi-stationary state. It is a result of the fact, that during the propagation through the low density supersonic wind the shock speed remains nearly constant. The analysis of the dynamical equations shows that in this case the CR distribution function has a selfsimilar form $f(r, p, t) = \Phi(r/R_s, p)/t^2$ (see Appendix) which is roughly consistent with the numerical results presented on Fig. 2a. It also explains the time constancy of the maximum particle momentum obtained by Völk & Biermann (1988), as mentioned in the Introduction..

A more detailed consideration includes the shock deceleration. In the case of the ejecta density described by the selfsimilarity distribution Eq. (9) at the early phase, when $V_s > v_t$, the expected expansion law is

$$R_s \propto \left(\frac{V_w}{\dot{M}} \right)^{1-\nu} t^\nu \quad (23)$$

with $\nu = (k - 3)/(k - 2)$ (Chevalier 1982), which in our case has the value $\nu = 0.875$. The decrease of the shock velocity

$$V_s = \nu \frac{R_s}{t} \propto t^{\nu-1} \quad (24)$$

leads to a decrease of the injection momentum $p_{inj} \sim mV_s \propto t^{\nu-1}$ that introduces an additional time dependent factor in the CR distribution function $f \propto p_{inj}^{q_s-3} \propto t^{(\nu-1)(q_s-3)}$ at least at nonrelativistic energies. It results in the dependence $f \propto t^{-\mu}$ where $\mu = 2\nu - (\nu - 1)(q_s - 3)$. In our case $k = 10$, $\sigma_s = 3.4$ this gives $q_s = 4.25$ and $\mu = 1.91$. Due to the selfregulating property of the nonlinear acceleration process, CR particles absorb some constant fraction of the shock energy; therefore at relativistic energies $f_s \propto \rho_s V_s^2 \propto t^{-2}$.

A direct consequence of this fact is the evolution of the overall, i.e. volume integrated CR spectrum

$$N(p, t) = 16\pi^2 p^2 \int_0^\infty dr r^2 f(r, p, t),$$

which is shown in Fig. 2c as a function of momentum p for five subsequent evolutionary phases. The shape of the spectrum and the value of the cutoff momentum p_m change slowly during the evolution. At high energies $10^2 \lesssim p/\text{mc} \lesssim 10^4$ the overall CR spectrum is close to the

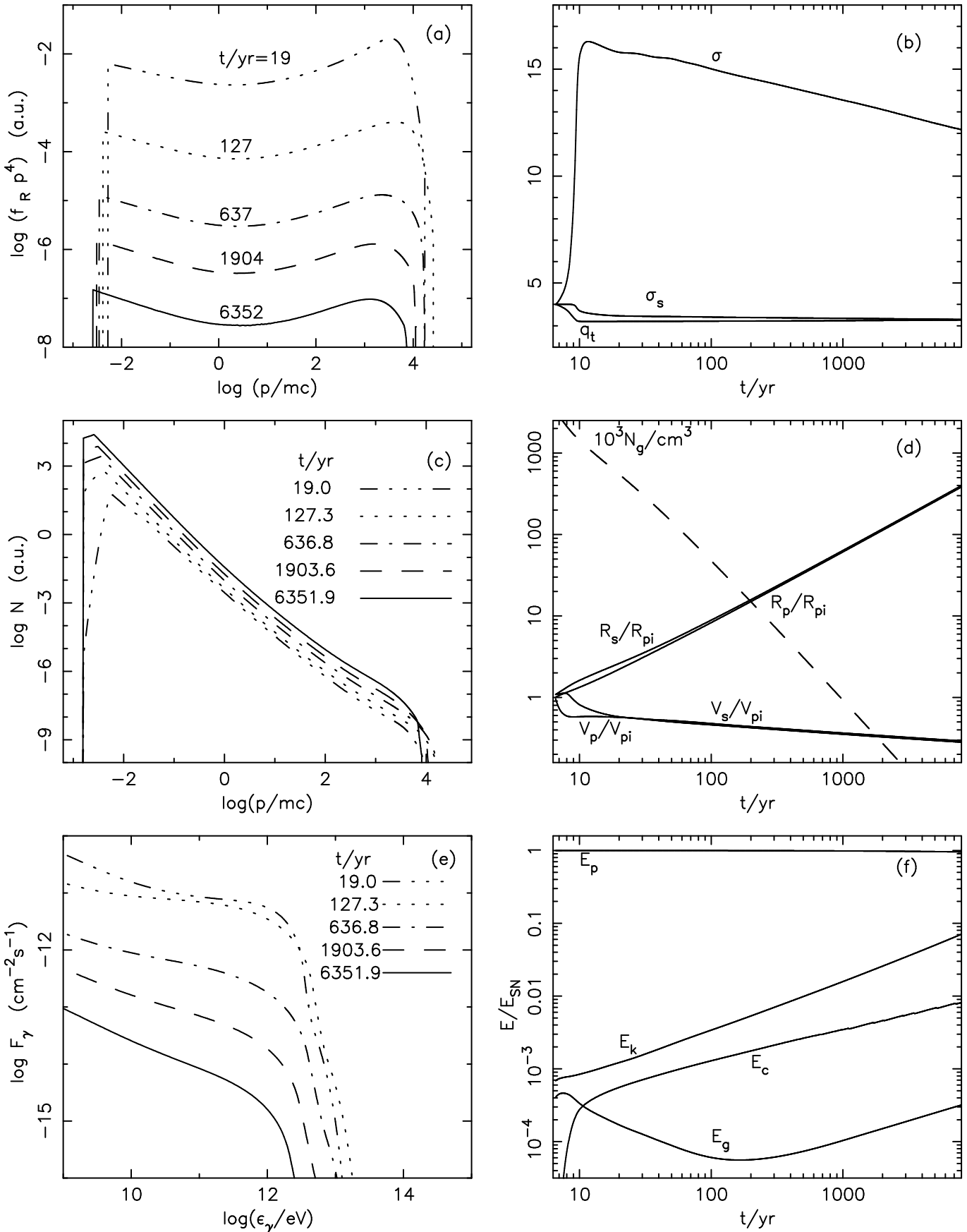


Fig. 2. CR and gas dynamics in a WR wind region. CR distribution function at the shock front (a), volume integrated overall CR spectrum (c), as functions of momentum, and overall integral γ -ray spectrum normalized to a distance of 1 kpc (e), as function of γ -ray energy, at five different times t . Total shock compression ratio σ , subshock compression ratio σ_s and differential power law index q_t (b). Shock (suffix s) and piston (suffix p) radii R_s and velocities V_s (full

form $N \propto p^{-1.5}$. It is interesting to note that the overall CR spectrum is even harder than the local CR spectrum at the shock front $n_s = 4\pi p^2 f_s(p)$, because the size of the upstream region $l = \kappa_s(p)/V_s$ occupied by CRs with momentum p is proportional to p . At relatively low momenta $l(p) \ll R_s - R_p$ and the overall spectrum $N(p)$ mainly consists of the CRs situated in the downstream region $R_p < r < R_s$; therefore in this case $N(p) \propto n_s(p)$. At high momenta $p \sim p_m$ diffusive length $l(p)$ becomes comparable with the downstream region size $R_s - R_p \approx R_s/(3\sigma)$; therefore the overall spectrum $N(p)$ becomes progressively harder with increasing p due to upstream region. The amplitude of the spectrum grows with time because the volume occupied by accelerated CRs increases with time $V \propto R_s^3$ that gives $N \propto V f_s p^2 \propto t^{3\nu-\mu}$. The index $3\nu - \mu$ varies from 0.72 at $p < mc$ to 0.63 at $p > mc$ in good agreement with the numerical results.

One can compare the calculated and the expected value of the CR cutoff momentum, which is determined by the expression (Berezhko 1996)

$$\frac{p_m}{mc} = \frac{R_s(V_s - V_w)}{A\kappa_s(mc)}, \quad (25)$$

where

$$A = [2 + 2b + e + d - (\nu - 1)/\nu] q_t / (5 - q_t), \quad (26)$$

and the parameter $d = (r\nabla w)_2 \sigma / [(\sigma - 1)V_s]$ describes the effect of particle adiabatic cooling in the downstream region, and the dimensionless parameters

$$\nu = d \ln R_s / d \ln t, \quad b = d \ln f_s / d \ln R_s, \quad e = \nu d \ln \kappa_s / d \ln R_s$$

describe the time variation of the shock radius, of the CR distribution function and of the CR diffusion coefficient, respectively. In addition

$$q_t = 3\sigma' / (\sigma' - 1) \quad (27)$$

is the lower limit for the power law index, and $\sigma' = (V_s - V_w - c_a)/u_2 = \sigma(1 - 1/M_a)$ is the effective total shock compression ratio which includes the effect produced by the outward propagation of Alfvén waves in the upstream region $r > R_s$. By definition the value of p_m is that momentum where the local power law index $q = -d(\ln f)/d(\ln p)$ drops to the value $q = 5$.

In the case under consideration the gas velocity w is almost constant in the downstream region, which gives $d = 2$ (Berezhko 1996). Taking into account that $R_s \propto t^{0.875}$, $f_s \propto t^{-2}$, $\kappa_s \propto R_s$ we have $\nu = 0.875$, $b = -2$, and $e = 0.875$, and the expression for the expected cutoff momentum can be written in the form

$$\frac{p_m}{mc} = 2.5 \times 10^4 \left(\frac{B_*}{50 \text{ G}} \right) \left(\frac{\Omega}{10^{-6} \text{ s}^{-1}} \right) \times \left(\frac{R_*}{3 \times 10^{12} \text{ cm}} \right)^2 \left(\frac{2 \times 10^3 \text{ km/s}}{V_w} \right) \left(\frac{t}{10 \text{ yr}} \right)^{-0.125} \quad (28)$$

which is in a good agreement with the numerical results (see Fig. 2a,c). Note that the main factors which determine the value of p_m are the adiabatic CR cooling in the expanding medium, the finite time increase of the shock size, and the decrease of the shock velocity, but not the time factor, as it is frequently assumed (e.g. Lagage & Cesarsky 1983).

During the time interval $t < 5922$ yr of shock propagation through region (a) of the supersonic wind CRs absorb only a small fraction of the explosion energy $E_c \approx 0.008E_{sn}$ (see Fig. 2f) due to the small amount of swept up matter $M_{sw} = 0.3M_\odot$ compared to the ejected mass $M_{ej} = 10M_\odot$, where

$$M_{sw} = 4\pi \int_0^{R_s} dr r^2 \rho, \quad (29)$$

$\rho(r)$ is the wind density, determined by the expression (12).

The γ -ray spectrum F_γ is shown in Fig. 2e. It is extremely hard in the energy range $10^{10} \lesssim \epsilon_\gamma \lesssim 10^{12}$ eV during the early phase $t < 500$ yr and becomes progressively steeper as time proceeds. This behavior is a consequence of the fact that the γ -ray flux $F_\gamma = F'_\gamma + F''_\gamma$ consists of two different parts. The first, F'_γ , is due to CR interaction with the swept-up matter which lies between the piston and shock surfaces and has the mass M_{sw} . In the case we consider here, the CRs are almost uniformly distributed in the downstream region $R_p < r < R_s$. Therefore we have approximately (Berezhko & Völk 1997)

$$F'_\gamma \propto M_{sw} e_{c2} p_m^{\gamma-2}, \quad (30)$$

where e_{c2} is the CR energy density in the downstream region. In our case $e_{c2} \propto \rho_s V_s^2$, $M_{sw} = \dot{M}R_s/V_w$, $\gamma \approx 1.7$, giving the expected dependence $F'_\gamma \propto t^{-1.1}$ which is in a agreement with the numerical results at $t > 10$ yr. The calculated γ -ray flux can be represented in the form

$$F'_\gamma(1 \text{ TeV}) = F'_{10} \times \left(\frac{d}{1 \text{ kpc}} \right)^{-2} \left(\frac{t}{10 \text{ yr}} \right)^{-1.1} \quad (31)$$

with $F'_{10} = 2 \times 10^{-12} \text{ cm}^{-2} \text{ s}^{-1}$, which is in rough agreement with the estimates of Berezinskii & Ptuskin (1989), and Kirk et al. (1995) which do not include CR penetration into the ejecta with subsequent γ -ray generation. The energy spectrum of this component $F'_\gamma \propto \epsilon_\gamma^{-0.6}$ is steeper than the CR integral spectrum, because upstream CRs interacting with the relatively low density medium contribute much less to the γ -ray spectrum than to the overall CR spectrum

The second part of γ -ray flux F''_γ has its origin in the ejecta material whose CR energy density is e_{c3} . Therefore we have

$$F''_\gamma \propto M_{ej} e_{c3} p_m^{\gamma-2}. \quad (32)$$

The ratio of the two components

$$F''_\gamma / F'_\gamma = (M_{ej}/M_{sw})(e_{c3}/e_{c2})$$

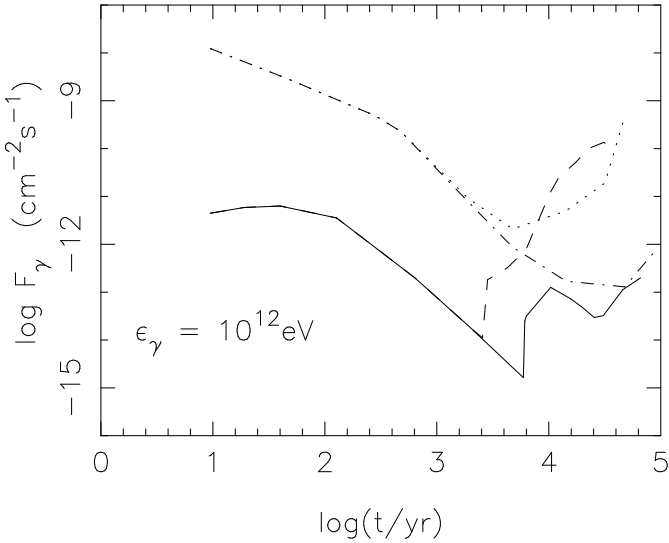


Fig. 3. Integral flux of γ -rays with energy $\epsilon_\gamma > 1$ TeV, normalized to a distance of 1 kpc, as a function of time for the cases of a SNR Ib with $N_H = 0.3 \text{ cm}^{-3}$ (full line), SNR Ib with $N_H = 30 \text{ cm}^{-3}$ (dashed line), SNR II with $N_H = 0.3 \text{ cm}^{-3}$ (dash-dotted line), and SNR II with $N_H = 30 \text{ cm}^{-3}$ (dotted line).

is determined by the two factors M_{ej}/M_{sw} and e_{c3}/e_{c2} . The swept up mass $M_{sw} = \dot{M}R_s/V_w$ increases with time and reaches the value $M_{sw} = 0.03M_{ej}$ at $t \sim 6000$ yr. At $t < 100$ yr the ratio e_{c3}/e_{c2} grows from zero to about 0.05 and then remains nearly constant. Therefore, during the initial period $t < 10^3$ yr, the γ -ray flux at $\epsilon_\gamma \sim 1$ TeV is dominated by the second component whereas at $t > 6000$ yr the first component becomes dominant at almost all energies.

Since $e_{c3} \propto \rho_s V_s^2 \propto t^{-2}$ at $t > 100$ yr we have $F''_\gamma \propto t^{-2}$ and numerically

$$F''_\gamma(1 \text{ TeV}) = 4.6 \times 10^{-12} \times \left(\frac{d}{1 \text{ kpc}} \right)^{-2} \left(\frac{t}{100 \text{ yr}} \right)^{-2} \frac{1}{\text{cm}^2 \text{s}}. \quad (33)$$

The second component $F''_\gamma(\epsilon_\gamma)$ is much harder than $F'_\gamma(\epsilon_\gamma)$ (see Fig. 2e) because CRs with higher energy penetrate into the piston more effectively. Therefore the expected flux $F_\gamma(\epsilon_\gamma)$ becomes progressively steeper as the contribution of F''_γ decreases with time (see Fig. 2e).

The time dependence of the expected integral flux of TeV γ -rays at the distance $d = 1$ kpc is shown in Fig. 3. It also includes the epochs when the SNR shock leaves the wind region and enters the bubble and the shell regions, to which we turn now.

For $t > t_1 = 5922$ yr the SN shock propagates through the hot region (b) of the MS bubble. When the SNR shock intersects the boundary $r = R_1$, which is also a strong discontinuity, a new secondary shock arises (Shigeyama & Nomoto 1990). It propagates several times between the

SNR shock front and the piston surface, and compresses and heats the medium. It thus provides the transition to the new quasi-stationary state which corresponds to the SNR shock propagating through region (b). We neglect this complicated transition phenomenon. We rather describe the beginning of the SN shock propagation in the region (b) in the following simplified manner. We start with a pure gas shock of size $R_s = R_p + 0$, piston size $R_p = R_1$ and piston speed $V_p = V_{p1} = 4127$ km/s which is the final piston speed in the region (a). We neglect the CRs produced during the previous period $t < t_1$. This underestimates the CR and γ -ray production in region (b). But the influence of previously produced CRs is not very large because the CR production rate increases sharply when the SNR shock intersects the boundary $r = R_1$, on account of the much higher gas density in region (b) (see Fig. 1).

Fig. 4 illustrates the dynamics of the system during this period.

Note that the CR distribution functions in Figs. 2a and 4a are measured in the same units; this is also the case for the overall CR spectra in Figs. 2c and 4c. One can see that already at $t = 6100$ yr the CR number density and the CR distribution function increase by more than two orders of magnitude compared to the time $t = t_1 = 5922$ yr. In the region (b) efficient CR acceleration lasts less than four thousands years: only for $t \lesssim 10^4$ yr the shock produces a CR spectrum that is relatively hard in the relativistic energy range (see Fig. 4a). For $t \gtrsim 10^4$ yr it becomes progressively steeper so that the CR number density at energy $\epsilon = 10$ TeV, which generates TeV-energy γ -rays, has already at $t = 3 \times 10^4$ yr decreased by more than two orders of magnitude. Due to this reason TeV-energy γ -rays at $t \gtrsim 10^4$ yr are produced by CRs accelerated at the earlier stage $t \lesssim 10^4$ yr, and the contribution of freshly accelerated CRs to the γ -ray production is negligible. The γ -ray flux decreases with time for $t \gtrsim 10^4$ yr because of adiabatic cooling of the CRs accelerated during the previous stage.

Due to its high temperature, region (b) is characterized by a relatively large value of the sound speed $c_s = 188$ km/s. When it breaks into the region (b) the shock has a velocity of about $V_s = 4500$ km/s. Therefore even the initial Mach number $M = 24$ is not very high. Only during an initial period $t \lesssim 10^4$ yr the shock compression ratio σ is substantially larger than 4 (see Fig. 4b), and high energy CRs are produced with relatively high efficiency. At later stages $t \gtrsim 10^4$ yr the shock decelerates rapidly (Fig. 4d) and becomes too weak to accelerate high energy CRs efficiently. Due to the small Mach number the total shock compression ratio σ at $t \gtrsim 10^4$ yr is less than 4 and even the lower limit q_t for the power law index at $t \gtrsim 10^4$ yr becomes greater than 5 (Fig. 4b). The CR spectrum $f_s \propto p^{-q}$ produced by the SN shock at this stage is very steep ($q \geq q_t > 5$) which is tantamount to a low acceleration efficiency.

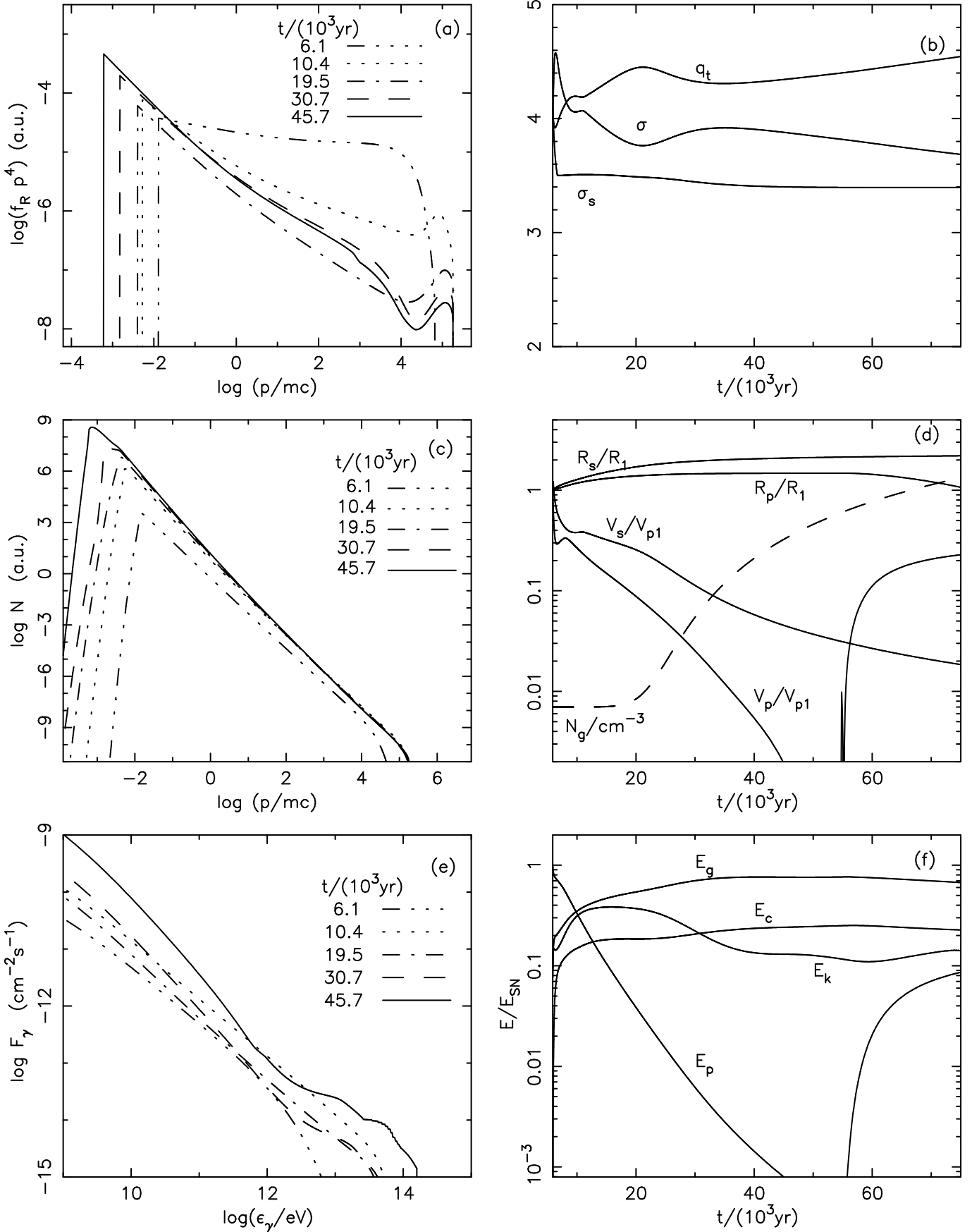


Fig. 4. The same as Fig. 2 but for SNR shock propagation through the WR bubble which was reached after 5922 yr. The normalization parameters in Fig. 4c are, respectively, $R_1 = 30.8 \text{ pc}$, $V_{p1} = 4127 \text{ km/s}$.

One can see from Fig. 4c that the number of high energy CRs with $p/mc \gtrsim 10^3$, produced in the SNR, increases only during the initial period $t \lesssim 10^4$ yr and then remains nearly constant during shock propagation in the bubble. The lower energy particles, on the other hand, continue to be accelerated beyond this time, steepening the overall spectrum at lower energies, whereas E_c remains nearly constant. At the end of this stage about 22 percent of the explosion energy is transformed into CRs (see Fig. 4f). Since the chemical composition of the bubble gas is more and more modified towards a pure interstellar composition the further out in radius the shock extends, we conclude from Fig. 4c that the chemical composition of the CR spectrum becomes more wind material-like (heavier) towards higher particle energies. The same tendency is seen in the later SN II case (see Fig. 5c). This effect is peculiar to wind SNe but it is only one of several factors which lead to an increasingly heavier chemical composition of the Galactic CRs with increasing particle energy.

Approximately, neglecting the mass in the wind, the behavior of CR and γ -ray production in the bubble is determined by the dynamical scale length l_0 and the corresponding time scale

$$t_0 = l_0/V_0, \text{ where } V_0 = \sqrt{2E_{sn}/M_{ej}}$$

is the mean ejecta velocity. As in the case of a uniform medium l_0 is the length over which the amount of swept-up material equals the ejected mass M_{ej} . The principal difference to the case of a uniform medium is that in the case of the bubble the shock expansion starts from the initial size $R_s \approx R_1$ which is much larger than l_0 .

Therefore the appropriate definition for the dynamic scale in the case under consideration is

$$l_0 = \frac{M_{ej}}{4\pi R_1^2 \rho_b}, \quad (34)$$

where ρ_b is the bubble density. It gives the value $l_0 = 4.92$ pc which is much smaller than R_1 . The corresponding time scale is $t_0 = 1522$ yr. One can see from Fig. 3 that in agreement with this time scale the TeV-energy γ -ray emission reaches its peak value $F_\gamma \approx 10^{-13} \text{ cm}^{-2}\text{s}^{-1}$ at $t \approx t_1 + 2t_0 \approx 10^4$ yr, that is at the beginning of the Sedov phase as in the case of a uniform ISM. Later on the γ -ray flux gradually decreases (see Fig. 3) due to the decrease of the CRs production because of the decrease of the shock strength (see Fig. 4b).

For a long time (at least up to $t = 8 \times 10^4$ yr) the CR energy content E_c remains nearly constant. In the case under consideration the adiabatic cooling of CRs is less important compared with the uniform ISM case because the shock size at the Sedov phase varies over a very small range: during the period from $t \approx 7 \times 10^3$ yr to $t \approx 7 \times 10^4$ yr the shock size increases only by a factor of two (see Fig. 4d).

At $t > 10^4$ yr the CR energy content at the shock front is mainly in the form of low energy particles because

freshly accelerated CRs are characterized by a progressively steeper spectrum (see Fig. 4a). Note that the local peak (bump) in $p^4 f_s(p)$ at $p \sim 10^5 mc$ represents the so-called escaping particles (Berezhko 1986a; Berezhko et al. 1996). Fig. 4c shows that the overall CR spectrum $N(p, t)$ in the relativistic energy range remains nearly constant for $t > 10^4$ yr. It has an almost pure power law form $N \propto p^{-2.1}$ in the momentum interval $10 \lesssim p/mc \lesssim 10^5$ (Fig. 4c).

The efficiency of high energy γ -ray production increases again for $t > 2 \times 10^4$ yr due to the increasing gas density (see Fig. 4e). But even at $t \sim 10^5$ yr, when $N_g(R_s) \sim 1 \text{ cm}^{-3}$ the TeV-energy γ -ray flux remains significantly lower than $10^{-12} \text{ cm}^{-2}\text{s}^{-1}$.

Note that during this stage the total number of high energy CRs remains almost constant since the shock becomes too slow and weak, and does not accelerate energetic particles any more. Nevertheless one can expect a significant increase of high energy γ -ray production later on when the strong population of previously produced CRs will expand outward and finally reach the shell (c) and its boundary. During this stage an almost constant number of CRs progressively interacts with an increasing amount of gas and this will lead to an increasing γ -ray production. Unfortunately, it is not simple to describe the dynamics of the system during this late stage. One has for example to expect a strong increase of the CR diffusion coefficient due to the decrease of the CR energy density as well as magnetohydrodynamic wave damping by ion neutral friction in the partially ionized shell gas. This suggests a much faster outward loss of CRs compared to the Bohm diffusion case, unless the SNR is surrounded by a hot, fully ionized gas which reflects the particle back across the shell.

In Fig. 3 we also present the time dependence of the TeV-energy γ -ray flux for the same case of a SNR Ib but for a higher (asymptotic) ISM number density $N_H = 30 \text{ cm}^{-3}$. In this case we have $R_1 = 14.6$ pc, $R_2 = 34.7$ pc, $N_b = 2.82 \times 10^{-2} \text{ cm}^{-3}$, $P_b = 1.1 \times 10^{-11} \text{ dyne/cm}^2$, $B_b = 16.7 \mu\text{G}$. One can see that the character of the SNR evolution is very similar to the previous case. For $t < 2544$ yr SN the shock propagates through the region (a) of the supersonic WR-wind and its evolution is initially identical to the previous case.

The bubble region, reached by the SNR shock at $t_1 = 2544$ yr, is characterized by the length scale $l_0 = 1.8$ pc and the time scale $t_0 = 555$ yr. The value $F_\gamma = 3 \times 10^{-13} \text{ cm}^{-2}\text{s}^{-1}$, reached at $t \approx t_1 + 2t_0 = 3654$ yr, would be the peak flux for a uniform medium with number density $N_0 = N_b$. In contrast to the previous case, the γ -ray flux continues to increase for $t > 3654$ yr because at this period the SN shock enters the region (c), where the gas density starts to increase rapidly (see Fig. 4d).

One can see from Fig. 3 that the γ -ray flux reaches the value $F_\gamma \approx 10^{-10} \text{ cm}^{-2}\text{s}^{-1}$ at $t \approx 3 \times 10^4$ yr. A comparison with the previous case shows that this peak flux scales as N_H as in the case of a uniform ISM (e.g. Berezhko &

Völk 1997). However, it is essentially lower (at least by a factor of 100) than in the case where the ISM is uniform with the same density N_H . The main reason of this low efficiency of γ -ray production is that in the case under discussion the majority of CRs is produced in the low density bubble. When the SN shock enters the high density shell region (c) it becomes weak and therefore an inefficient CR accelerator. In this phase, in comparison with the case of a uniform ISM, the same amount of CRs mainly produced at previous evolutionary phases generates a much lower γ -ray flux because of the poor spatial overlap between the CR and gas distributions (see Berezhko & Völk 1997). The peak of the gas density distribution lies just behind the shock front, whereas the CRs are sitting deeper inside where the density of the gas is much lower.

3.2. Type II supernova

We model the type II SN case as a progenitor star with initial mass $15M_\odot$ (e.g. Leitherer et al. 1992) that spends a time period $\Delta t_w = 4 \times 10^6$ yr on the main-sequence with a mass-loss rate $\dot{M} = 2.5 \times 10^{-7} M_\odot \text{ yr}^{-1}$ and wind velocity $V_w = 2000 \text{ km/s}$, and then the time $\Delta t_w = 10^5$ yr in the RSG phase with mass-loss rate $\dot{M} = 2 \times 10^{-5} M_\odot \text{ yr}^{-1}$ and wind velocity $V_w = 15 \text{ km/s}$. The MS wind creates a bubble of size $R_2 = 61 \text{ pc}$ in the ISM with $N_H = 0.3 \text{ cm}^{-3}$. According to Eqs. (14) and (15) the bubble is characterized by $N_b = 6.6 \times 10^{-3} \text{ cm}^{-3}$ and $P_b = 4.4 \times 10^{-13} \text{ dyne/cm}^2$.

The RSG wind occupies the region of size $R_f = V_w \Delta t_w = 1.54 \text{ pc}$. At this point the ram pressure ρV_w^2 of RSG wind exceeds the thermal pressure P_b in the bubble. Therefore we neglect the shell which can be formed in the RSG wind due to its interaction with the ambient bubble material. We model the transition zone between the RSG wind and the bubble by the set of parameters $\rho = \rho(R_f)(R_f/r)^{3.5}$, $V_w = V_w(R_f)(R_f/r)^2$. We introduce this zone to match smoothly the gas densities N_g between regions (a) and (b), see Fig. 1. It contains a small amount of gas and plays no role in the overall SNR evolution.

We use a magnetic field strength $B = 2 \times 10^{-4} \text{ G}$ in the RSG wind at the distance $r = 10^{17} \text{ cm}$. It formally correspond to $B_* = 1 \text{ G}$, $R_* = 3 \times 10^{13} \text{ cm}$ and $\Omega = 3 \times 10^{-8}$. Our B-field is about 60 times smaller than that assumed by Völk & Biermann (1988). Their magnetic field implies an Alfvén velocity c_a which is considerably larger than the wind speed V_w . This renders the existence of the RSG mass outflow as a supersonic wind problematic (Axford 1994). In our case the RSG wind is superalfvénic with $c_a \approx 0.5V_w$. It might be possible to model a slow outflow starting with a much higher stellar magnetic field which is then subalfvénic. However, we shall not attempt such a dynamical construction in this paper.

We start the computation of the SNR evolution with the initial conditions $t_i = 3.17 \text{ yr}$, $R_{pi} = 10^{17} \text{ cm}$, $V_{pi} = 10^4 \text{ km/s}$.

Fig. 5 illustrates SN shock evolution, CR and γ -ray production for an ISM with $N_H = 30 \text{ cm}^{-3}$. The character of the CR spectrum $f_s(p, t)$, shown in Fig. 5a, and of the overall CR spectrum $N(p, t)$, plotted in Fig. 5c, are similar to the previous case of the SN Ib for $t < 500$ yr when the SN shock propagates through the region (a) of the supersonic wind. The value of the cutoff momentum $p_m \approx 2 \times 10^5 \text{ mc}$ is consistent with formula (28). The acceleration efficiency and the corresponding shock modification are very high. During the initial stage $t \approx 10 \text{ yr}$ the shock compression ratio reaches the value $\sigma = 15$ and then slowly decreases due to the shock deceleration (see Fig. 5b). As a consequence the high energy part of the CR spectrum is extremely hard $N \propto p^{-1.2}$ at $10^3 \lesssim p/\text{mc} \lesssim 10^5$.

It is interesting to note that the γ -ray spectrum $F_\gamma \propto \epsilon_\gamma^{-0.5}$ (Fig. 5e) is much steeper at $10^{11} \lesssim \epsilon_\gamma \lesssim 10^{13} \text{ eV}$ than the integral CR spectrum: the CRs in the upstream region $r > R_s$, which make the integral CR spectrum extremely hard, play a much less important role in the formation of the γ -ray spectrum, because they occupy a relatively lower density region.

In the present case the γ -ray generation within the ejecta is negligible. Therefore, according to relation (30), the expected γ -ray flux $F_\gamma(1 \text{ TeV})$ should be about 5×10^3 times larger than the flux $F'_\gamma(1 \text{ TeV})$ in the case of the WR wind. One can see from Fig. 3 and Fig. 5e, that the calculated γ -ray flux can be represented in the form (31) with $F_{10} = 1.2 \times 10^{-8} \text{ cm}^{-2} \text{s}^{-1}$ in agreement with relation (30).

During these initial 500 years the SN shock sweeps up $M_{sw} = 2M_\odot$, CRs absorb about 10% of the explosion energy (see Fig. 5f) and the expected γ -ray flux $F_\gamma(1 \text{ TeV})$ exceeds the value $10^{-10} \text{ cm}^{-2} \text{s}^{-1}$ (see Fig. 3).

During the period $500 < t < 1000$ yr the SN shock propagates through the intermediate zone (see Fig. 5d) which contains only a small amount of matter. The CR energy content slowly increases, but the CR spectrum becomes progressively steeper. Together with the decrease of the gas density this leads to a decrease of the γ -ray flux $F_\gamma \propto t^{-2}$ (see Fig. 3).

For $t > 10^3$ yr the SN shock propagates through the bubble whose characteristics are similar to the bubble around the progenitor of a type Ib SN, in an ISM with the same density N_H (see Fig. 1). Therefore at this stage the expected γ -ray production continues to decrease up to the time $t = 4 \times 10^3$ yr, when the γ -ray production by CRs accelerated during previous stages drops to a level that corresponds to a flux $F_\gamma \sim 10^{-12} \text{ cm}^{-2} \text{s}^{-1}$ typical for a uniform medium with $N_0 = N_b$. For $t > 4 \times 10^3$ yr γ -rays produced in the bubble material start to dominate and the γ -ray flux increases with time. At $t = 10^4$ yr the SN shock reaches the shell region (c) where the density increases. Therefore the expected γ -ray flux increases more rapidly for $t > 10^4$ yr (see Fig. 3), even though the CR production becomes quite low in this phase (see Fig.

5f). More than 40% of the explosion energy goes into CRs during the full SNR evolution.

In Fig. 3 we present also the calculated γ -ray flux $F_\gamma(1 \text{ TeV})$ for the case $N_H = 0.3 \text{ cm}^{-3}$. The time-dependence of $F_\gamma(1 \text{ TeV})$ for $t < 2 \times 10^3 \text{ yr}$ is identical to the previous case. For $t > 2 \times 10^3 \text{ yr}$ the SN shock propagates through the bubble whose characteristics are now similar to the case of a type Ib SNR with $N_H = 0.3 \text{ cm}^{-3}$. Therefore, the expected γ -ray production during late phases $t > 10^4 \text{ yr}$ is close to that case (see Fig. 3).

4. Summary

Our numerical results show that when a SN explodes into a circumstellar medium strongly modified by a wind from a massive progenitor star, then CRs are accelerated in the SNR almost as effectively as in the case of a uniform ISM (Berezhko et al. 1994, 1995, 1996; Berezhko & Völk 1997): about 20 \div 40% of the SN explosion energy is transformed into CRs during the active SNR evolution.

During SN shock propagation in the supersonic wind region very soon the acceleration process reaches a quasi-stationary level which is characterized by a high efficiency and a correspondingly large shock modification. Despite the fact that the shock modification is much stronger than predicted by a two-fluid hydrodynamical model (Jones & Kang 1992), the shock never becomes completely smoothed by CR backreaction: a relatively strong subshock always exists and plays an important dynamical role. As in the case of a uniform ISM, the spurious complete shock smoothing in hydrodynamic models is the result of an underestimate of the role of geometric factors.

Due to the relatively small mass contained in the supersonic wind region CRs absorb there only a small fraction of the explosion energy (about 1% in the case of a SN type Ib, and 10% in the case of a SN type II) and the SNR is still very far from the Sedov phase after having swept up this region. Therefore we conclude, that the CRs produced in this region should not play a very significant role for the formation of the observed Galactic CR energy spectrum.

The peak value of the CR energy content in the SNR is reached when the SN shock sweeps up an amount of mass roughly equal to several times the ejected mass. This takes place during the SN shock propagation in the modified bubble. In a purely adiabatic bubble the sweep-up would occur at the beginning of the shell. Compared with the uniform ISM case the subsequent adiabatic CR deceleration is less important in the case of a modified circumstellar medium. The main amount of CRs in this case is produced when the SN shock propagates through the bubble. In this stage the dynamical scale length is much smaller than the shock size. Therefore the relative increase of the shock radius during the late evolution stage and the corresponding adiabatic effects are small. These configurational properties lead to potentially interesting changes

of the CR chemical composition with particle energy (see Sect. 3.1)

In the case of the modified circumstellar medium the CR and γ -ray spectra are more variable during the SN shock evolution than in the case of a uniform ISM (Berezhko & Völk 1997). At the same time the form of the resulting overall CR spectrum is rather insensitive to the parameters of the ISM as in the case of uniform ISM. The reason is that the main amount of CRs are produced in the latest phase which has still a strong enough shock. Roughly speaking, the overall CR spectrum (except the most energetic CRs) is mainly formed at the stage when the shock compression ratio lies between 4 and 5.

The maximum energy of the accelerated CRs reached during the SNR evolution is about 10^{14} eV for protons in all the cases considered.

Our results confirm the important conclusion, reached for the case of a uniform ISM before, that the diffusive acceleration of CRs in SNRs is able to generate the observed CR spectrum up to an energy $\sim 10^{14} \text{ eV}$, if the CR diffusion coefficient is as small as Bohm limit. This disregards the possibility of turbulent field amplification, as discussed in Sect. 2.

In the case of a SN Ib the expected TeV-energy γ -ray flux, normalized to a distance of 1 kpc, remains lower than $10^{-12} \text{ cm}^{-2} \text{s}^{-1}$ during the entire SNR evolution if the ISM number density is less than 1 cm^{-3} except for an initial short period $t < 100 \text{ yr}$ when it is about $10^{-11} \text{ cm}^{-2} \text{s}^{-1}$. Only for a relatively dense ISM with $N_H = 30 \text{ cm}^{-3}$ the expected γ -ray flux is about $10^{-10} \text{ cm}^{-2} \text{s}^{-1}$ at late phases $t > 10^4 \text{ yr}$. A similar situation exists at late phases of SNR evolution in the case of SN II. It is interesting to note that the expected γ -ray flux is considerably lower, at least by a factor of hundred, compared with the case of uniform ISM of the same density N_H . This confirms the preliminary result reported earlier (Berezhko & Völk 1995)

The type II SN explodes into the dense wind of the red supergiant progenitor star. During the first several hundred years t_m after the explosion, the expected TeV-energy γ -ray flux at a distance $d = 1 \text{ kpc}$ exceeds the value $10^{-9} \text{ cm}^{-2} \text{s}^{-1}$ and can be detected up to the distance $d_m = 30 \text{ kpc}$ with present instruments like HEGRA, Whipple or CAT. This distance is of the order of the diameter of the Galactic disk (see also Kirk et al. 1995). Therefore all Galactic SNRs of this type whose number is $N_{sn} = \nu_{sn} t_m$ should be visible. But in this case we can expect at best $N_{sn} \sim 10$ such γ -ray sources at any given time.

The typical value of the cutoff energy of the expected γ -ray flux is about 10^{13} eV , if the CR diffusion coefficient is as small as the Bohm limit. In this respect the negative result of high-threshold arrays (Borione et al. 1995; Allen, G.E. et al. 1995; Allen, N.H. et al. 1995) in searching of γ -ray emission from Galactic SNRs is not surprising because their threshold $E_{th} \sim 50 \text{ TeV}$ exceeds the cutoff energy of the expected γ -ray flux; marginally this also holds

for the negative results of the lower threshold $E_{th} > 20$ TeV AIROBICC array (Prahl & Prosch 1997; Prosch et al. 1996). It is less obvious how to interpret the negative results of imaging atmospheric Cherenkov telescopes with thresholds less than about 1 TeV (Mori et al. 1995; Lessard et al. 1997; Hess et al. 1997; Hess 1998; Buckley et al. 1998). For core collapse SN of types II or Ib with quite massive progenitors one can in part explain this fact by the extremely low π^0 -decay γ -ray intensity expected from such SNRs during the period of SN shock propagation through the low-density hot bubble. An alternative possibility relates to the assumption of the Bohm limit for the CR diffusion coefficient which can be too optimistic, in particular for the quasi-perpendicular geometry in wind-blown regions from rotating stars. For a slightly more general discussion of SNR γ -rays in stellar wind cavities, see Völk (1997).

Acknowledgements. This work has been supported in part by the Russian Foundation of Basic Research grant 97-02-16132. One of the authors (EGB) gratefully acknowledges the hospitality of the Max-Planck-Institut für Kernphysik where part of this work was carried out under grant 05 3HD76A 0 of the Verbundforschung A&A of the German BMBF.

Appendix A: Similarity solution

Consider a shock of radius $R_s = V_s t$ that expands with constant speed V_s into the wind region, whose parameters are described by expressions (12), (13). We introduce the similarity variables

$$x = r/R_s,$$

$$f(r, p, t) = \Phi(x, p)/t^2,$$

$$P_c(r, t) = \Pi_c(x)/t^2,$$

$$w(r, t) = W(x),$$

$$\rho(r, t) = \Omega(x)/t^2,$$

$$P_g(r, t) = \Pi_g(x)/t^2.$$

Then the diffusive transport equation for the CR distribution function, eq.(1), and the gas dynamic equations (2)-(4) can be written in the form

$$\begin{aligned} 2\Phi + x \frac{\partial \Phi}{\partial x} &= \frac{1}{x^2 V_s} \frac{\partial}{\partial x} x^2 K \frac{\partial \Phi}{\partial x} - \frac{W}{V_s} \frac{\partial \Phi}{\partial x} + \\ &\quad \frac{1}{x^2 V_s} \frac{\partial}{\partial x} (x^2 W) \frac{p}{3} \frac{\partial \Phi}{\partial p} + \frac{\eta(V_s - W_1)\Omega_1}{4\pi m p_{inj}^3 V_s} \delta(x - 1), \\ \frac{\partial}{\partial x} [(xV_s - W)\Omega] - \frac{2W\Omega}{x} - 3V_s\Omega &= 0, \\ (xV_s - W)\Omega \frac{\partial W}{\partial x} &= \frac{\partial}{\partial x} (\Pi_g + \Pi_c), \end{aligned}$$

$$(W - xV_s) \frac{\partial \Pi_g}{\partial x} + \frac{\gamma_g}{x^2} \frac{\partial}{\partial x} (x^2 W) \Pi_g = \alpha_a (\gamma_g - 1) c_a \frac{\partial \Pi_c}{\partial x},$$

taking into account that in the wind region the Alfvén speed c_a is constant and small compared with the shock speed V_s , and plausibly assume that the CR diffusion coefficient has the form $\kappa(r, p, t) = K(x, p)R_s$. The boundary conditions do not contain the time explicitly. Therefore the above similarity solution is appropriate. The only factor which violates these assumptions it is the initial condition for CRs, which contains the time $t = t_i$ in explicit form. Therefore the exact solution will deviate from the similarity solution only during some short initial period of several t_i , as long as the shock speed is constant.

References

Allen G.E., Berley D., Biller S. et al., 1995 Proc. 24th ICRC (Roma) 2, 443
Allen N.H., Bond L.A., Budding E., et al., 1995 Proc. 24th ICRC (Roma) 2, 447
Atoyan A.M., Aharonian F.A. 1996, MNRAS 278, 525
Axford W.I. 1994, ApJS 90, 937
Axford W.I., Leer E., Skadron G. 1977, Proc. 15th ICRC (Plovdiv) 11, 132
Baring M.G., Ellison D.C., Reynolds S.P., Grenier I.A., Goret P. 1999, ApJ 513, 311
Bell A.R. 1978, MNRAS 182, 147; MNRAS 182, 443
Bennett L., Ellison D.C. 1995, J. Geophys. Res. 100, A3, 34439
Berezhko E.G. 1986a, Proc. Int. School & Workshop on Plasma Astrophysics (Sukhumi) (ESA SP-251-ISSN 0379-6566) 271
Berezhko E.G. 1986b, Pis'ma Astron. Zh. 12, 842
Berezhko E.G. 1996, Astropart. Phys. 5, 367
Berezhko E.G., Ellison D.C. 1999, ApJ, 526, 385
Berezhko E.G., Ellison D.C. 2000, ApJ, to be published
Berezhko E.G., Krymsky G.F. 1988, Soviet Phys. Uspekhi. 12, 155
Berezhko E.G., Völk H.J. 1995, Proc. 24th ICRC (Roma) 3, 380
Berezhko E.G., Völk H.J. 1997, Astropart. Phys. 7, 183
Berezhko E.G., Krymsky G.F., Turpanov A.A. 1990, Proc. 21st ICRC (Adelaide) 4, 101
Berezhko E.G., Yelshin V.K., Ksenofontov L.T. 1994, Astropart. Phys. 2, 215
Berezhko E.G., Ksenofontov L.T., Yelshin V.K. 1995, Nuclear Phys. B (Proc. Suppl.) 39A, 171
Berezhko E.G., Yelshin V.K., Ksenofontov L.T. 1996, JETP 82, 1
Berezinsky V.S., Ptuskin V.S., 1989, Sov. Astron. Lett. 14, 304
Berezinsky V.S., Bulanov S.V., Ginzburg V.L., Dogiel V.A., Ptuskin V.S. 1990, in *Astrophysics of Cosmic Rays*, North-Holland Elsevier Science Publ. B.V., Amsterdam Biermann P.L. 1993, A&A 271, 649; 1993, A&A 277, 691
Blandford R.D., Eichler D. 1987, Phys. Rept. 154, 1
Blandford R.D., Ostriker J.P. 1978, ApJ 221, L29
Borione A., Catanese M., Covault C.E., et al., 1995 Proc. 24th ICRC (Roma) 2, 439
Buckley J.H., Akerlof C.W., Carter-Lewis D.A., et al. 1998, A&A 329, 639

Chevalier R.A. 1982, *ApJ* 259, 302
 Chevalier R.A., Liang E.P. 1989, *ApJ* 344, 332
 Chuvilgin L.G., Ptuskin V.S. 1993, *A&A* 279, 278
 de Jager O.C., Harding A.K. 1992, *ApJ* 396, 161
 Dorfi E.A. 1990, *A&A* 234, 419
 Dorfi E.A. 1991, *A&A* 251, 597
 Drury L.O'C. 1983, *Rep. Prog. Phys.* 46, 973
 Drury L.O'C. 1984, *Adv. Space Res.* 4, 185
 Drury L.O'C., Markiewicz W.J., Völk H.J. 1989, *A&A* 225, 179
 Drury L.O'C., Aharonian F.A., Völk H.J. 1994, *A&A* 287, 959
 Drury L.O'C., Völk H.J., Berezhko E.G. 1995, *A&A* 299, 222
 Ellison D.C., Reynolds S.P., Borkowsky K., et al., 1994, *PASP* 106, 780
 Ellison D.C., Baring M.G., Jones F.C. 1995, *ApJ* 453, 873
 Garcia-Segura G., Langer N., Mac Low M.-M. 1996, *A&A* 316, 133
 Giacalone J., Burgess D., Schwartz S.J., Ellison D.C. 1993, *ApJ* 402, 550
 Hess M., for the HEGRA coll'n 1997, *Proc. 25th ICRC (Durban)* 3, 229
 Hess M. 1998, PhD Thesis Univ. Heidelberg
 Jokipii J.R. 1997, *ApJ* 313, 842
 Jones T.W., Kang H. 1992, *ApJ* 396, 575
 Jones E.M., Smith B.W., Straka W.C. 1981, *ApJ* 249, 185
 Kahn F.D., Breitschwerdt D. 1989, *MNRAS* 242, 209
 Kang H., Jones T.W. 1991, *MNRAS* 249, 439
 Kirk J.G., Duffy P., Ball L. 1995, *A&A* 293, L37
 Kirk J.G., Duffy P., Gallant Y.A. 1996, *A&A* 314, 1010
 Krymsky G.F. 1964, *Geomag. Aeron.* 4, 977
 Krymsky G.F. 1977, *Soviet Phys. Dokl.* 23, 327
 Lagage P.O., Cesarsky C.J. 1983, *A&A* 125, 249
 Le, M.A. 1982, *J.Geophys. Res.* 87, 5063
 Leitherer C., Robert C., Durissen L. 1992, *ApJ* 401, 596
 Lessard R.W., Boyle P.J., Bradbury S.M., et al., 1997 *Proc. 25th ICRC (Durban)* 3, 233
 Losinskaya T.A. 1991, *Proc. 22th ICRC (Dublin)* 5, 123
 Lucek S.G. & Bell A.R., 2000, *Mon. Not. R. Astron. Soc.*, in press
 Bell A.R., Lucek S.G., 2000, *Mon. Not. R. Astron. Soc.*, submitted
 Malkov M.A. 1997, *ApJ* 485, 638
 Malkov M.A., Völk H.J. 1995, *A&A* 300, 605
 Malkov M.A., Völk H.J. 1996, *Adv. Space Res.* 21, No. 4, 551
 Markiewicz W.J., Drury L.O'C., Völk H.J. 1990, *A&A* 236, 487
 Mastichiadis A. 1996, *A&A* 305, L53
 Mastichiadis A., de Jager O.C. 1996, *ApJ*, 311, L5
 McKenzie J.F., Völk H.J. 1982, *A&A* 116, 191
 Mori M., Hara T., Hayashida N., et al., 1995 *Proc 24th ICRC (Roma)* 2,487
 Ostrowski M. 1988, *MNRAS* 233, 257
 Parker E.N. 1965, *Planet. Space Sci.* 13, 9
 Prahl J., Prosch C. 1997 *Proc 25th ICRC (Durban)* 3, 217
 Prosch C., Feigl E., Karle A., et al., 1996, *A&A* 314, 275
 Quest K.B. 1988, *JGR* 93, 9649
 Reynolds S.P. 1998, *ApJ* 493, 375
 Shigeyama T., Nomoto K. 1990, *ApJ* 360, 242
 Trattner K.J., Scholer M., 1991, *Geophys. Res. Lett.* 18, 1817
 Trattner K.J., Möbius E., Scholer M. et al., 1994, *JGR* 99, 389
 Völk H.J., 1984, in *Proc. 19th Recontre de Moriond Astrophysics Meeting: "High Energy Astrophysics"* (ed. J. Tran Thanh Van), editions Frontieres, Gif-sur-Yvette, France, p. 281 ff
 Völk H.J. 1997, in: *Towards a Major Atmospheric Cherenkov Detector* - V, O.C. de Jager (ed.), Kruger Park, p.87 ff
 Völk H.J., Biermann P.L. 1988, *ApJ* 333, L65
 Völk H.J., Drury L. O'C., McKenzie J.F., 1984, *A&A* 130, 19
 Weaver R., McCray R., Castor J. et al., 1977, *ApJ* 218, 377

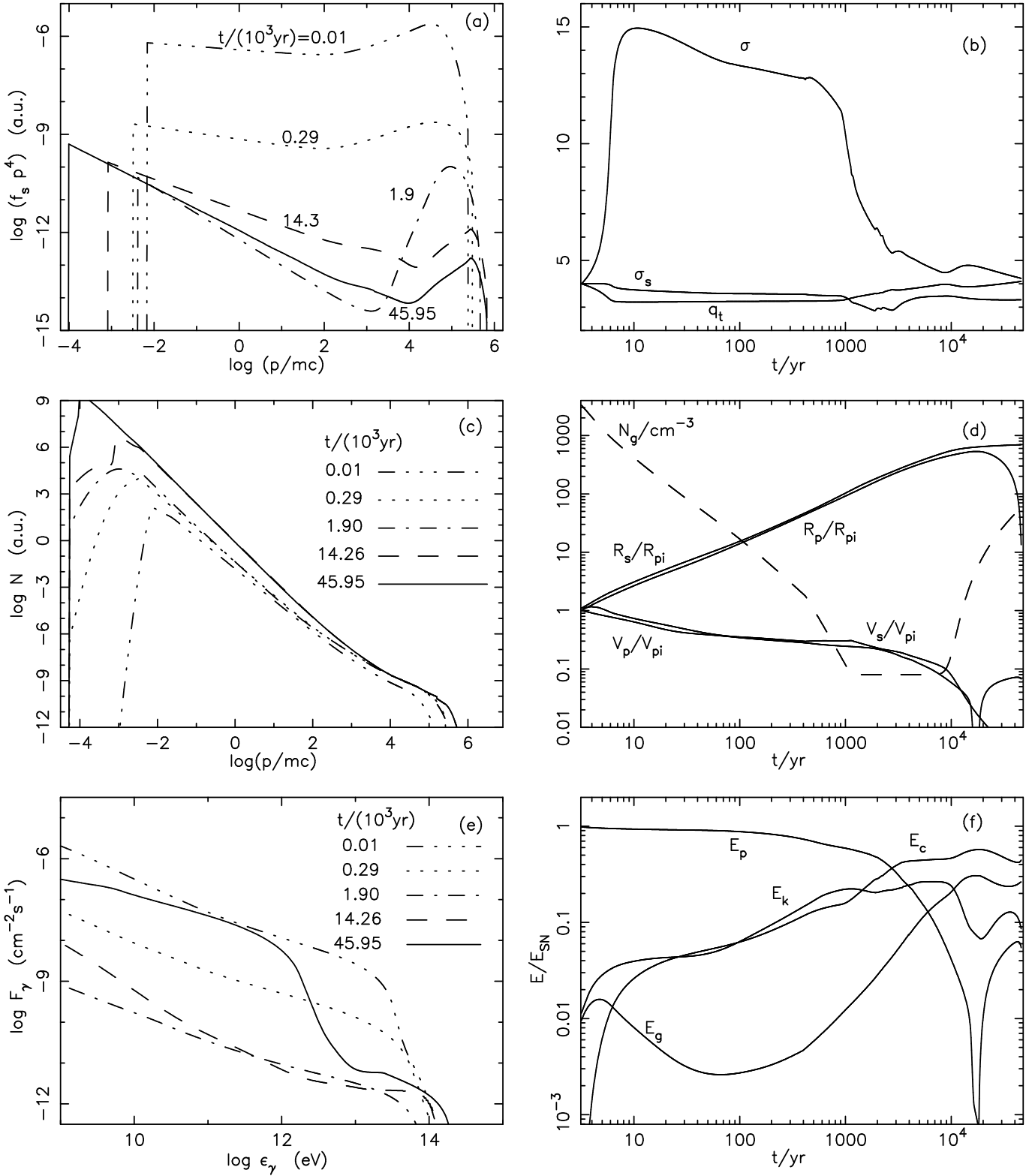


Fig. 5. The same as Fig. 2 but for the case of the remnant of a type II SN in an ISM with the hydrogen number density $N_H = 30 \text{ cm}^{-3}$, and encompassing the entire SNR evolution. The normalization parameters are, respectively, given by $R_{pi} = 10^{17} \text{ cm}$, $V_{pi} = 10^4 \text{ km/s}$